고효율 전력변환장치를 사용한 연료전지 시스템의 토폴로지

문상필, 서기영, 이현우, 권순걸, M.Nakaoko, 신휘범*
경남대학교, 경상대학교*

Topology of High Efficiency Power Conversion with Fuel Cell Generation System

S. P. Mun, K. Y. Suh, H. W. Lee, S. K. Kwon, M. Nakaoko, H. B. Shin*
Kyung-nam University, Gyeong-Sang National University*

Abstract - In this study paper, a 3[kW] Fuel Cell Generation (FCG)system with Fuel Cell(FC)simulator has been proposed. The developed FC simulator generates the actual voltage and current output characteristics of the Proton Exchange Membrane Fuel Cell (PEMFC), so that the overall performance and the dynamics of the proposed system could be effectively examined and tested. In this paper, at first, the system configuration and operational principle of the developed FC simulator has been investigated and the design process of the FCG system is explained in detail. In addition, the validity of the proposed system has been verified by the informative simulation and experimental results.

1. INRODUCTION

At the beginning of the 21st century, fuel cells meet the power needs of a variety of applications. The Fuel Cell(FC)is electrochemical device that converts chemical energy directly into electrical and thermal energy. The basic features of a FC system are composed of six basic subsystems : a fuel cell stack, a fuel processor, an air, water, and thermal management, and Power Conditioner System(PCS). The overall systems promise to provide a number of advantages, such as diversity of fuels, high efficiency at full and part-load, comparability of wide range of sizes, and independence of environmental pollution.

Although, a FC system is regarded as one of the preferable power sources with high- energy conversion efficiency, considering the environmental problems associated with energy consumption, it still suffers from its high price and complexity of peripheral devices. Due to high price and operational complicity of the FC stack, researchers have difficulty on development of a proper PCS, which consisted of a DC-DC boost converter, a bi-directional DC-DC converter, and a DC-AC inverter. With this problem, until now, even though many PCS have been developed and reported, they are mainly tested with constant DC source, not FC stack.

Therefore, the actual performance and dynamics of the PCS, considering of nonlinear V-I characteristic of the FC, could not be examined. A solution, which can develop the Fuel Cell Generation(FCG)system without using an actual FC stack, is highly desired especially for the first stage of development. With these requirements, several types of the FC simulator have been reported.

With the help of the presented simulators, in this paper, an advanced FC simulator has been proposed and a 3[kW] Proton Exchange Membrane FC (PEMFC) generation system has been developed and tested. The proposed FC simulator has some advantages over the conventional simulators on simple hardware construction, simple control algorithm, and fast response for the load variations. The hardware configuration and operational principle of the proposed FC simulator have been explained in detail and simulation results are provided in order to verify the validity of the developed FCG system.

2. A Fuel-Cell Generation System with The Proposed Fuel-Cell Simulator

2.1 Basic Operations of PEMFC

The basic fuel cell concept involves converting chemical energy directly into electrical energy. It produces electricity by electrochemically combining fuel(hydrogen)and oxidant(oxygen from the air) gases through electrodes and across an ion-conducting electrolyte. The fuel cell is composed of two electrodes, an anode, cathode, the catalyst, and an electrolyte, as illustrated in Fig. 1.

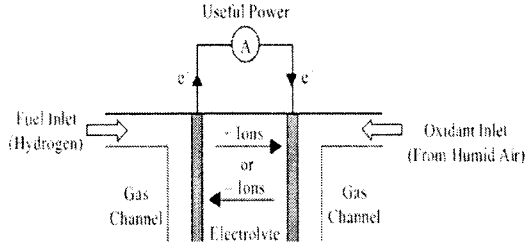

Fig. 1 Fuel Cells Basic Configuration.

The PEMFC is one of the most promising fuel cell types, and is often considered a potential replacement for the internal combustion engine in transportation applications. The PEMFC consists of porous carbon electrodes bound to a thin sulphonated polymer membrane. The anode, cathode, and net cell reactions of the PEMFC can be represented as

$$\text{Anode Reaction} : H_2 \quad 2H^+ + 2e^- \tag{1}$$

$$\text{Cathode Reaction} : 1/2O_2 + 2H^+ + 2e^- \quad H_2O \tag{2}$$

$$\text{Net Cell Reaction} : H_2 + 1/2O_2 \quad H_2O \tag{3}$$

where the mobile ion is H^+. The membrane electrode assembly (MEA)is sandwiched between two collector plates that provide an electrical path from the electrodes to the external circuit. Flow channels cut into the collector plates distribute reactant gases over the surface of the electrodes. Individual cells consisting of collector plates and MEAs are assembled in series to form a fuel cell stack.

2.2 System Description and Circuit Design

Fig. 2 shows the detailed circuit of the proposed high efficiency power conversion for fuel cell generation System. The DC-DC conversion stage of this architecture consists of two fuel cells employing boost converters, a super-capacitor employing bi-directional buck-boost converter

and a low voltage DC-bus capacitor. An additional DC-DC converter of push-pull type are employed.

At the initial start-up, two fuel cells charge the super-capacitor through the MOSFET S_{2a} and DC-bus capacitor as well. Under normal operating conditions, two boost converters supply 10[%] of the rated power to the load. However, when the load changes suddenly, the fuel cell generation system is not able to respond promptly to the power demand change due to its delay time for fuel flow rates to adjust. In this situation, the system controls the switch S_{3a} to supply the DC-bus by the boost operation. This control topology is also useful for handling the instantaneous over-load situation. If the load demands more than the rated power momentarily, the stored energy in the super-capacitor can be utilized to supply the load, thereby preventing the fuel cell from being over-loaded. It is obvious that system delay or voltage drop is unavoidable without this auxiliary power system in the condition os sudden load change and/or over-load. The DC-AC conversion stage of this architecture consists of IGBT inverter module and produces the high quality sinusoidal 240[V] output voltage based.

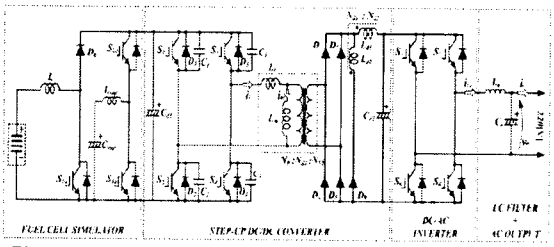

Fig. 2 Circuit of the proposed high efficiency power conversion for fuel-cell generation system.

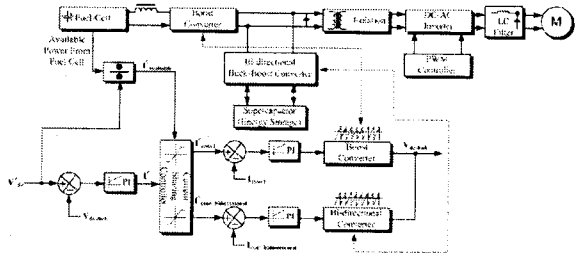

Fig. 3 Block diagram of the system control.

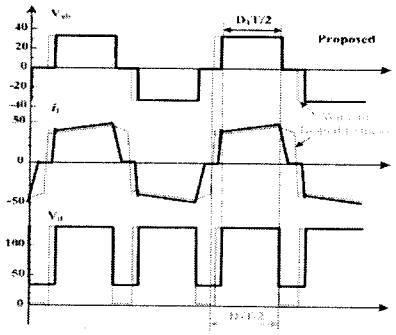

Fig. 4 Operation waveforms of PS-PWM DC-DC converter.

Fig. 3 shows the block diagram of DC-DC boost converter scheme. In the figure DC-DC converter are combined with fuel cells, and bi-directional buck-boost converter is combined with a super -capacitor. The control scheme is combined of one voltage control loops and two independent current control loops and the DC-bus voltage is controlled by a PI controller to generate the system current command. Power available signal from the fuel cell indicates the available power from the fuel cell at the moment and thereby available current command is calculated.

In the situation of a power shortage or instantaneous overload current sharing controller calculates the appropriate current command values for each converter and sends it to them. Fig. 4 shows the operation waveforms of the proposed PS-PWM DC-DC power converter with the tapped inductor filter compared to the conventional ZVS PS-PWM DC-DC power converter without tapped inductor.

In case of the proposed DC-DC converter to achieve the same power in the output with the conventional DC-DC converter, the duty cycle D_1 ($D=t_{on}/T$) is smaller than duty cycle D_2 of the conventional converter. It means that to achieve the same power in the output the DC source must be connected to the output through DC-DC converter circuit shorter time and it is prove that the circulating current can be reduced. The operation during the next half-cycle is symmetrical with the mentioned above half-cycle and does not shown. As described above the switches S_1 and S_2 are turned on and turned off with ZVS, while the switches S_3 and S_4 operate with ZCS at turn-on and turn-off. The circulating current during the freewheeling interval t_0-t_4 is substantially lowered. As was shown above, the tapped inductor L_{d1}/L_{d2} in the proposed soft-switching PS-PWM DC-DC power converter operates as a smoothing inductor and also makes that the rectified output voltage v_d is clamped to the value $v_d=\alpha_L E_0$ during the freewheeling interval. Therefore, the clamped voltage $v_d=\alpha_L E_0$ is applied during the freewheeling interval to the transformer leakage inductance L_l and reset its energy to zero. As result during the freewheeling interval, the output current flows through the additionally connected freewheeling diode D_9.

The using tapped inductor filter L_{d1}/L_{d2} with connected freewhee -ling diode makes possible to reduce the circulating current without using any active switches and theirs driver circuit. Fig. 5 shows the rectified voltage v_d waveform. During a half cycle period, the rectified voltage v_d is expressed as,

$$\left\{ \begin{array}{lll} v_d = N_L E_0 & \text{for} & t_0 < t \le t_4 \\ v_d = \dfrac{E}{N_T} & \text{for} & t_4 < t \le t_5 \end{array} \right\} \quad (4)$$

The output voltage characteristic equation of the proposed DC-DC power converter can be represented by,

$$E_0 = \frac{DE}{\alpha_T\{1-\alpha_L(1-D)\}} - \frac{L_s I_0}{\alpha_T^2 T_h \{1-\alpha_L(1-D)\}^2} \quad (5)$$

To make the average output voltage E_0 characteristic independent of the output current I_0, and to obtain effective cancellation of the circulating current, the leakage inductance Ls of the high frequency transformer is designed as small as possible.

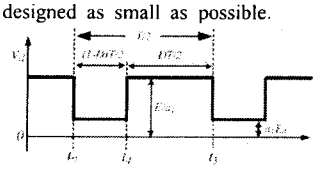

Fig. 5 Operating waveform of rectified voltage v_d.

Fig. 6 shows the Full-bridge DC-AC inverter, which generates single-phase 220/60[Hz] AC voltage. The controller consists of a DSP, which processes voltage feedback signal, and an I/O control unit. Output voltage of the inverter is controlled to be constant voltage and constant frequency with the help of sinusoidal PWM(SPWM)control scheme.

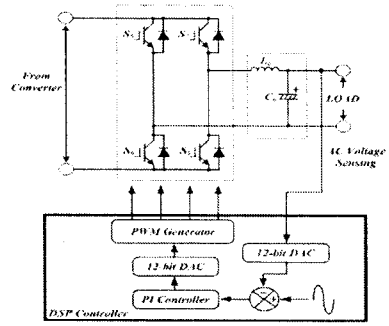

Fig. 6 Block diagram of single-phase DC-AC inverter

The output filter of the power inverter is used to smooth out the waveforms generated from our DC-AC stage. If monitored, the pure output of the inverter is a square-wave with varying duty cycles. This signal contains many unwanted frequencies including multiples of the 4.5[kHz] PWM switching frequency. Total harmonic distortion(THD) can be affected by these harmonics, therefore, the THD of the inverter can be reduced by using an output filter. The THD requirement for this design requires the system to have a THD < 5[%]. This low-pass filter is designed to meet the THD and power requirements of this project. The following section will describe the procedure used to find the appropriate values of the components of the filter. Fig. 7 below shows the topology for the output filter. A transfer function is developed from the schematic. The assumptions used in the analysis are, the output filter is loss less and the third current harmonic current is 80[%]of the fundamental current frequency.

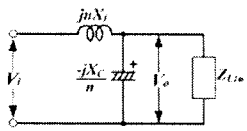

Fig. 7 Topology of the DC-AC output filter.

3. Simulation and Experimental Results

Table 1 shows the design parameters of proposed fuel-cell generation system. Fig. 8 shows its dynamic output characteristics.

When the load current changed from 20[A] to 50[A], the transient response is plotted in Fig. 8. Then, the stack is stabilized to 50[A] and 46[V] after approximately 0.05[s]. Of course, since the electrochemical reaction time of Fuel Cells is short time constant, the transient actually shows how the load reacts to a specific change.

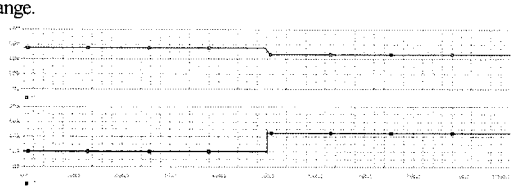

(a) Without time constant

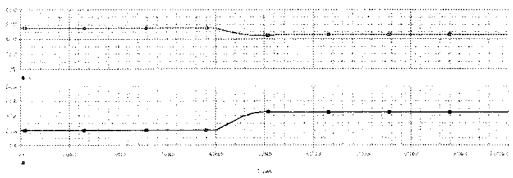

(b) With time constant

Fig. 8 Current voltage transient simulation results of the proposed circuit.

Table. 1 Design specifications and circuit parameters.

Fuel-Cell	Input Voltage(Vs)	39 ~ 60[VDC]
	inductor	L = 1[mH]
	Super-capacitor	C_{sup} = 1.66[F]
	Super-inductance	L_{sup} = 500[uH]
	Output capacitor( )	C_{d1} = 250[uF]
DC-DC Converter	MOSFET'S	S_{1a}~S_{2a} / S_1~S_4(2SK3228) V_{DS}=80[V], R_{DS}=0.006, I_{DS}=75[A]
	Diodes	D_0 / D_5~D_9(30JL2C41) V_{RRM}=600[V], I_0=30[A]
	Lossless snubber capacitors	C_1~C_4 = 30[nF]
	Transformer turns ratio	a_T = 1 : 13
	Leakage inductance	L_l = 300[nH]
	Magnetizing inductance	L_m = 70[uH]
	Tapped inductor	L_{d1} = 50[uH], L_{d2} = 13[uH] (Tapped inductor turns ratio a_L = 0.3)
	Output capacitor( )	C_{d2} = 250[uF]
Inverter	MOSFET'S	S_5~S_8(2SK3228) V_{DS}=80[V], R_{DS}=0.006, I_{DS}=75[A]
	Output Power(P_0)	3.0[kW]
	Output Voltage(V_0)	220[VAC]
	Switching Frequency	fs = 4.5[kHz]
	Output inductance	L_0 = 900[uH]
	Output capacitance	C_0 = 20[uF]

Fig. 9 illustrates switching pulse sequences and theoretical operating voltage and current waveforms of the presented converter at steady state. The switches S_1 and $S_2$are driven complementary with the blanking interval t_d. This interval t_d is needed to obtain the ZVS commutation of the switches $S_1$and S_2 at the turn-on instant. The dead time of the switches S_3 and S_4 is designed from consideration of the switching power devices and theoretically does not need for soft-switching operation of these switches. The output voltage of the proposed DC-DC converter is regulated by lagging the gate pulse of the switch $S_4(S_3)$ with respect to the gate pulse of the switch $S_1(S_2)$ and varying by this way an interval t_{on} (t_{on}=DT/2) as PS-PWM control with the constant switching frequency f=1/T. The simulated waveforms of the transformer primary side current i_l, inductor L_{d1} current i_{Ld2}, and rectified voltage v_d are shown at Fig. 10. The design of the tapped inductor L_{d1}/L_{d2} turns ratio a_L is made on the basis of the simulation results under the closed

loop control scheme(see Fig. 10).

Fig. 11 shows the output characteristics according to the lad variation of FC simulator. Fig. 11(a) shows the voltage-current waveforms when load current changed from 20[A] to 50[A] with not having the time delay function, and Fig. 11(b) represents output characteristics with time delay function.

To verify the operating principle of the proposed soft-switching PS-PWM DC-DC power converter and to evaluate its steady state characteristics, the laboratory level experiment is carried out with a 3[kW] circuit prototype. To achieve high efficiency and high performance of the DC-DC converter the low voltage power MOSFETs are selected as the power active switching devices.

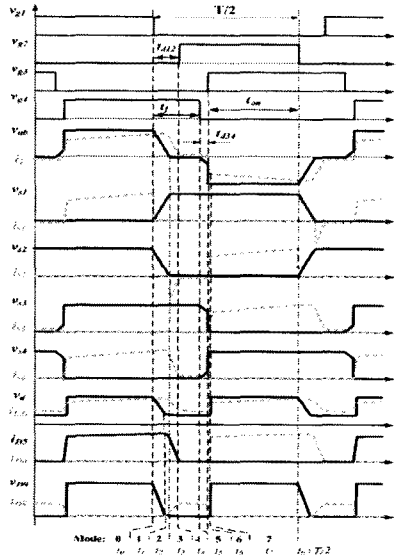

Fig. 9 Operation waveforms of the proposed soft-switching PS-PWM DC-DC converter.

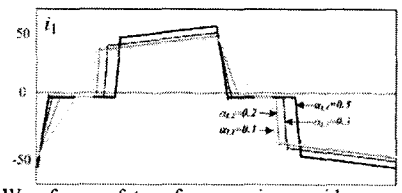

(a) Waveforms of transformer primary side current i_1

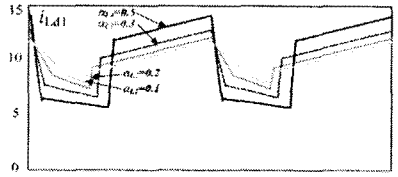

(b) Waveforms of filter inductor L_{d1} current i_{Ld1}

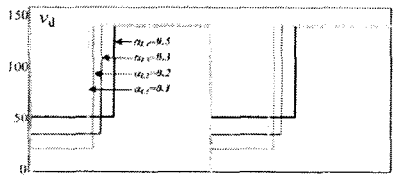

(c) Waveforms of the rectified voltage v_d

Fig. 10 Calculated results under closed loop control scheme.

The power circuit components parameters are indicated at the Table 1. Fig. 12(a) and (b) illustrate the measured voltage and current waveforms of the high frequency transformer Tr at 15[%] light and 100[%] full load, respectively. Fig. 13(a), (b) and Fig. 14(a), (b) show the measured voltage and current waveforms and power switches S_2 and S_4 at light and full load, respectively. It is obvious that the circulating current is suppressed during freewheeling interval, and the primary current flows through transformer only when DC source voltage is applied to the transformer. Moreover, the switch $S_2(S_1)$ operates with ZVS, switch $S_4(S_3)$ operate with ZCS at turn-on and turn-off as demonstrated at Fig. 13(a), (b) and Fig. 14(a), (b) at 15[%] light and 100[%] full load. The measured waveforms of the rectified voltage v_d and freewheeling diode D_9 current i_{D9} are presented at Fig. 15.

The output voltage E_o characteristics of the tested DC-DC power converter as a function of the output current Io under different duty cycle value D are shown at Fig. 15.

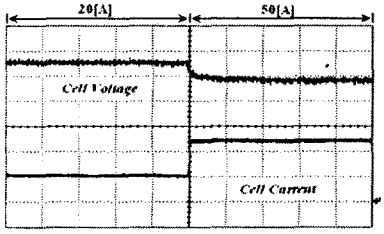

(a) Without time constant(10[V/div], 20[A/div])

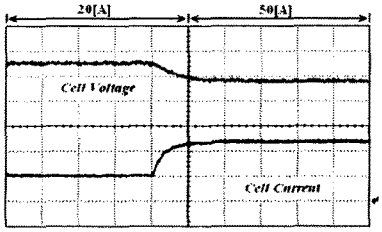

(b) With time constant(10[V/div], 20[A/div])

Fig. 11 Current voltage transient experimental results of the proposed circuit.(50[ms/div])

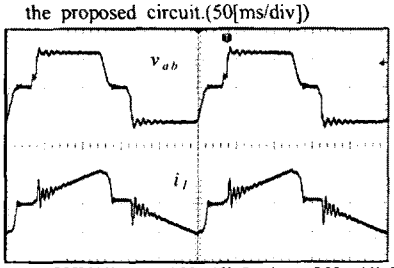

(a) v=50[V/div], i=10[A/div], time=20[μs/div]

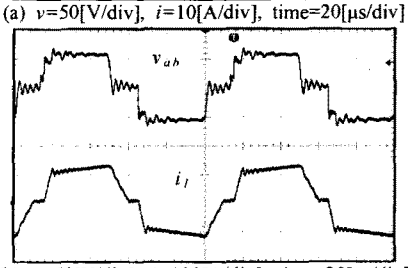

(b) v=50[V/div], i=100[A/div], time=20[μs/div]

Fig. 12 High-frequency transformer Tr voltage v_{ab} and current i_1 waveforms

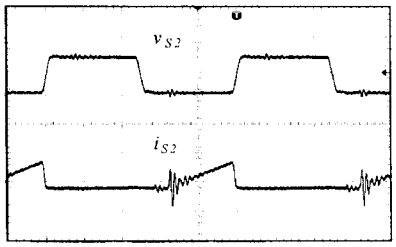

(a) v=50[V/div], i=10[A/div], time=20[μs/div]

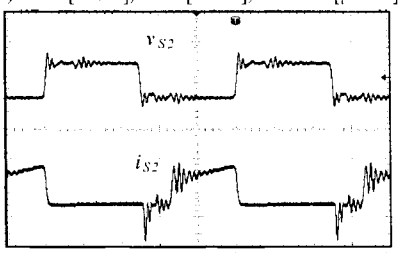

(b) v=50[V/div], i=100[A/div], time=20[μs/div]

Fig. 13 Voltage and current waveforms of switch S_2

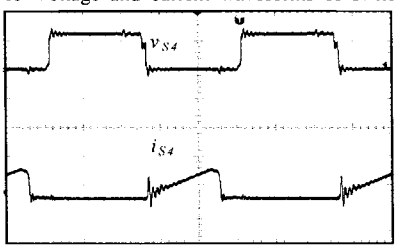

(a) v=50[V/div], i=10[A/div], time=20[μs/div]

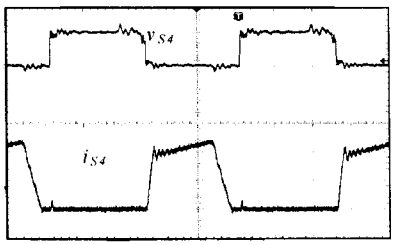

(b) v=50[V/div], i=100[A/div], time=20[μs/div]

Fig. 14 Voltage and current waveforms of switch S_4

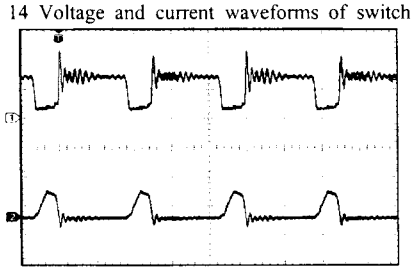

(v=50[V/div], i=10[A/div], time=20[μs/div])

Fig. 15 Measured waveforms of the rectified voltage v_d and freewheeling diode D_9 current i_{D9}

The corresponding experimental voltage and current responses of the fuel cell and inverter output terminals at 3.0[kW] resistive load are depicted in Fig. 16. From the experimental results, the favorable regulation performance of the inverter ac output voltage under the fuel cell variant DC voltage can be obtained. By observing the fuel cell current waveform, the current ripple within 120[Hz], which is caused by the ac load component, can be diminished by the utilization of a series of electrolytic capacitors with lower equivalent series resistance(ESR) values.

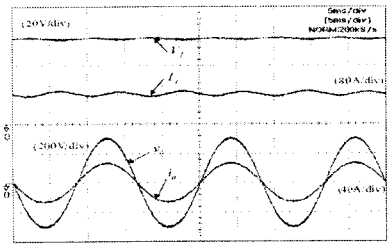

Fig. 16 Experimental voltage and current responses of fuel cell and inverter output terminals at 3.0[kW] resistive load

ACKNOWLEDGMENT

This work was supported by the Korea Research Foundation Grant funded by the Korean Government (MOEHRD) (KRF- 2005-037- D00006)

4. Conclusion

This study has been successfully developed a high efficiency power conversion strategy via voltage clamping and soft-switching methodologies for a PEM fuel cell generation system. By way of experimental validation, all switches and diodes in this circuit were operated with soft-switching characteristics, the inductor volume in the current-source circuit was smaller than the tradition one, and the voltage stress across switches was clamped down effectively.

The novel tapped inductor filter assisted high frequency transformer full-bridge soft-switching phase-shift PWM control scheme DC-DC power converter with ZVS and ZCS bridge-legs has been presented in this paper. The generation of the conduction power losses during freewheeling period caused by using phase-shift PWM control scheme and presence of the high frequency transformer leakage inductance has been suppressed due to make use of the tapped inductor filter with freewheeling diode in the converter output stage. The high efficiency stable soft-switching operation ability of the proposed DC-DC power converter has been verified on the basis of the experimental results using 3[kW]/17[kHz] prototype circuit.

Moreover, the measured THD improvement of the proposed power conversion system with respect to the commercial one was 0.87[%] at no load, 1.41[%] at *RL* load, 0.66[%] at sudden step load, and more than 2[%] at nonlinear load. In addition, the maximum efficiency of the proposed current source voltage inverter was measured over 95[%].

As a result, the proposed FC simulator can be a string method to relieve the difficult task on the development of PCS for FC applications.

REFERENCES

[1] Eun-Soo Kim, Yoon-Ho Kim, "An improved soft-switching PWM FB DC/DC converter for reducing conduction losses", IEEE Trans. on PE, Vol.14, No.2, pp.258-263, 1999.

[2] J.G.Cho, "Novel Zero-Voltage and zero-current-switching Full Bridge PWM Converter Using Transformer Auxiliary Winding", IEEE Trans. on PE, Vol.15, No.2, pp.250-257, 2000.

[3] National Oceanic and Atmospheric Administration: Climate of 2001, Annual Review.